Modification and Application of a New Method for Retrieving Water-Cloud Microphysics Vertical Profile

F.-L Chang and Z. Li
Earth System Science Interdisciplinary Center
University of Maryland
College Park, Maryland

Z. Li
Department of Meteorology
University of Maryland
College Park, Maryland

X. Dong
Department of Atmospheric Sciences
University of North Dakota
Grand Forks, North Dakota

Introduction

Low-level boundary layer clouds have the most significant influence on cloud radiative forcing due to their areal extent and frequent occurrence (Hartman et al. 1992). Radiation absorbed by the boundary layer clouds also plays an important role in cloud evolution and affects water redistribution (Stephens 1999). Since cloud morphological properties are an ensemble of cloud microphysics and cloud optical properties are governed by cloud microphysical properties, the most fundamental cloud variables are cloud microphysics, which influence the radiative transfer, droplet growth and precipitation processes in clouds.

Satellite observations provide the only means of acquiring global and long-term cloud droplet effective radius (DER) measurements. Some knowledge of the DER has been gained primarily by means of the AVHRR 3.7-μm data (e.g., Kaufman and Nakajima 1993; Han et al. 1994; Platnick and Twomey 1994; Nakajima and Nakajima 1995). Since the 3.7-μm measurement is over-sensitive to the absorption occurred near the cloud top, its DER retrieval does not represent the entire cloud column (Platnick 2000; Chang and Li 2002). To date, the moderate-resolution imaging spectroradiometer (MODIS) offers numerous advances that can improve the retrieval of cloud properties, like on-board calibrations and high spectral and spatial resolutions, among many others (King et al. 1992, 2003). This paper exploits the utility of the MODIS near infrared (NIR) measurements at 1.6, 2.1, and 3.7 μm for the retrieval of the DER vertical profile (DVP) using the method of Chang and Li (2002) and two modified methods. A preliminary validation is provided by comparing the MODIS satellite-based DVP retrievals to the ground-based retrievals using cloud-profiling radar and microwave radiometer measurements at the Atmospheric Radiation Measurement (ARM) Southern Great Plains (SGP) site in the North Central Oklahoma.

Three Analytic DER Vertical Profiles

Cloud property retrievals are commonly based on homogenous cloud models, i.e., where the DER is invariant with height. However, both theoretical studies (e.g., Platnick 2000) and observational data (e.g., Miles et al. 2000) suggest that the cloud DER often varies monotonically between cloud top and cloud base. NIR reflectances at multispectral wavelengths such as 1.6 µm, 2.1 µm and 3.7 µm can have different penetration path lengths into the cloud and convey certain information concerning the DVP (Platnick 2000; Chang and Li 2002). This information alone is insufficient to allow for the retrieval of any DER profile without a priori knowledge of the vertical weightings of the reflectance (Platnick 2000). To overcome this difficulty, Chang and Li (2002) assumed a linear DVP (hereafter referred to as DVP1) where the DER (r_e) is linearly proportional to the optical depth (τ') within the cloud, i.e., $r_e \propto \tau'$, where $\tau' = \tau/\tau_c$ and τ_c denotes the cloud optical depth.

Since many cloud measurements have suggested that r_e is more likely a linear function of the geometrical height (z), the DVP is modified accordingly (hereafter referred to as DVP2) such that $r_e \propto z'$, where $z' = z/z_c$ and z_c is the cloud vertical thickness. A third DVP (referred to as DVP3) is also studied where the assumption is that the cloud liquid water content (w) changes linearly with height, i.e., $w \propto z'$, which is the case for clouds formed from adiabatic processes. It is shown in Chang and Li (2003) that for the case of DVP1: $r_e \propto \tau'$ and $r_e \propto z'^{-1}$; for the case of DVP2: $r_e \propto z'$ and $r_e \propto \tau'^{1/3}$; and for the case of DVP3: $r_e \propto z'^{1/3}$ and $r_e \propto \tau'^{1/5}$ (e.g., Szczodrak et al. 2001).

In this study, we followed Platnick (2000) and adopted the three analytic DVPs, which were given as functions of τ' by, respectively,

$$\text{DVP1:}\quad r_e(\tau') = r_{e1} + (r_{e2} - r_{e1})\,\tau', \tag{1}$$

$$\text{DVP2:}\quad r_e(\tau') = [r_{e1}^3 + (r_{e2}^3 - r_{e1}^3)\,\tau']^{1/3}, \tag{2}$$

$$\text{DVP3:}\quad r_e(\tau') = [r_{e1}^5 + (r_{e2}^5 - r_{e1}^5)\,\tau']^{1/5}, \tag{3}$$

where r_{e1} is the DER at the cloud top ($\tau' = 0$) and r_{e2} is the DER at the cloud base ($\tau' = 1$). Note that Eq. 3 for the DVP3 is deduced from the original assumption given by

$$w(z') = w_1 + (w_2 - w_1)\,z', \tag{4}$$

where w_1 is the cloud-top LWC and w_2 is the cloud-base LWC. As shown in the Chang and Li (2003), $w \propto r_e^3$ and τ is proportional to $z^{5/3}$ for such a DVP.

For a vertically inhomogeneous DVP, the 3.7-µm reflectance depends mainly on the top layer of the cloud and is determined by r_{e1}. The less absorbing and shorter wavelengths like the 1.6-µm or 2.1-µm reflectances have more bearing deeper within the cloud and are determined by r_{e2}. The different dependencies of the three NIR reflectances on r_{e1} and r_{e2} lay the foundation for the retrieval of an optimal DVP (Chang and Li 2002).

Determination of Precipitable Water above Cloud

In satellite retrievals of DER, the amount of precipitable water (PW) above cloud is needed for calculating the water vapor attenuation. Conventionally, the above-cloud PW was determined based on some reanalysis data (e.g., National Centers for Environmental Prediction) derived at different scale and time or using estimates from some standard atmospheric model. Here a split window technique is adopted for the retrieval of above-cloud PW. The retrieval principle lies in varying strength of water vapor absorption at 11 μm and 12 μm, such that the difference in their brightness temperatures (brightness temperature difference [BTD] = T11 − T12) can be used to estimate the above-cloud PW for each 1-km pixel.

Figure 1 shows the BTD as a function of the above-cloud PW (g/cm^2) for various conditions of satellite viewing zenith angle (θ), cloud optical depth (τ_c), DER, and temperatures of the cloud top (T_c) and atmospheric profile. The results were calculated based on MODTRAN 4 with a water cloud layer inserted between 0.5 km to1.0 km. It is seen that a positive correlation between the BTD and above-cloud PW, which depends largely on θ (Figure 1a) and on cloud properties like τ_c (Figure 1b) and r_e (Figure 1c) and temperatures of cloud top (T_c), ground surface (T_g), and the atmosphere (Figure 1d). The dependences diminishes as τ_c increases (cf., $\tau_c = 1$ and 8 as seen in Figures 1b-1d). When $\tau_c = 8$, all dependences are less significant. In Figure 1d, note that the atmospheric temperature profile was modeled with a fixed lapse rate of $\Gamma = 6.5$K/km, hence $T_c = T_g - 6.5$K for a cloud-top height at 1 km.

The split-window PW retrieval scheme was applied to the Terra MODIS Level-1B 1-km data gathered at the ARM SGP site for two uniform stratus cloud systems observed on April 16 (1725 Universal Time Coordinates [UTC]) and May 31 (1655 UTC), 2001. Figure 2 shows the frequency distributions of (a) cloud-top temperature (T_c) and (b) above-cloud PW retrieved from a (30 km)^2 area centered at the SGP site. Our retrievals of T_c agree well with the ground-based measurements of mean $T_c = 262.2$ K on April 16 and 281.9 K on May 31. The cloud-top height (z_c) was about 4.87 km and 1.50 km, respectively, as indicated by ARM SGP balloon-borne radiosondes released at 1731 UTC, April 16 and at 1736 UTC, May 31 at Lamont, Oklahoma (36.61°N, 97.49°W). In our retrievals, z_c was calculated as $z_g + (T_g - T_c)/\Gamma$, where T_g was 289.6 K (April 16) and 290.6 K (May 31) according to the MODIS surface temperature product. Since $z_g = 0.31$ km for the SGP site, the mean z_c was calculated to be 4.53 km and 1.65 km, which were close to the radiosonde measurements. As for above-cloud PW, ARM-measured values were 0.14 g/cm2 from the radiosonde data and 0.16 g/cm^2 (1700 UTC) and 0.17 g/cm^2 (1800 UTC) from the microwave radiometer (MWR) retrievals on April 16 and were 1.15 g/cm^2 from the radiosonde data and 0.97 g/cm^2 (1600 UTC) and 0.87 g/cm^2 (1700 UTC) from the MWR retrievals on May 31. Our MODIS-retrieved mean PWs above cloud were 0.20 g/cm^2 for April 16 and 0.83 g/cm^2 for May 31; both agreed well with the ARM measurements, especially the MWR-based estimates. It is widely known that the magnitude of MWR-based column PW estimates is more reliable than the radiosonde (e.g., Guichard et al. 2000; Turner et al. 2003).

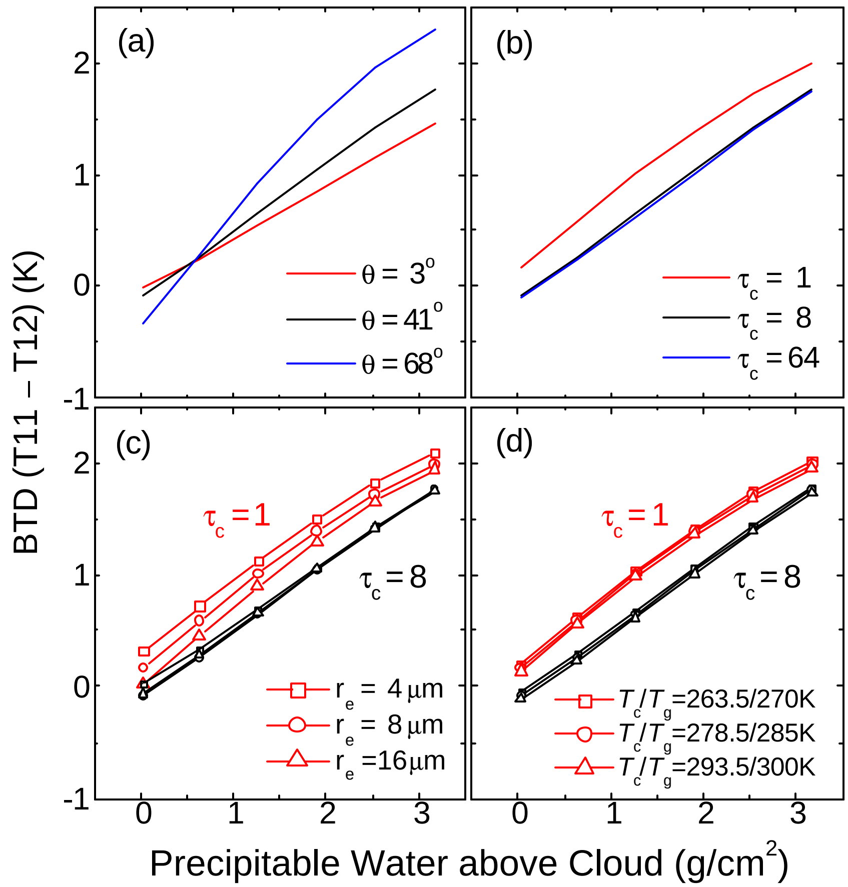

Figure 1. Model-simulated BTD versus the above-cloud PW for (a) three θ (τ_c = 8, r_e = 8 μm and T_c/T_g = 278.5/285K); (b) three τ_c (θ = 41.1°, r_e = 8 μm and T_c/T_g = 278.5/285K); (c) three r_e with τ_c = 1 and 8 (θ = 41.1° and T_c/T_g = 278.5/285K); and (d) three T_c/T_g with τ_c = 1 and 8 (θ = 41.1° and r_e = 8 μm).

DER Vertical Profiles Retrieved from MODIS

In retrieving the DVP, an iterative retrieval scheme similar to the conventional DER retrieval scheme was employed, except that (1) a DER profile determined by r_{e1} and r_{e2} was retrieved, instead of a constant r_e and (2) the above-cloud PW was retrieved during the iterative procedure. With initial guesses, the iterative procedure started by retrieving τ_c from the visible (0.64-μm) channel, followed by the retrievals of r_{e1} and r_{e2} from the three NIR channels, above-cloud PW from the split-window channels, and T_c from the 11-μm channel. The retrieval procedure was repeated until an acceptable level of convergence was achieved. Note that in retrieving the DVP, a two-channel retrieval technique was employed (Chang et al. 2002; Chang and Li 2003), which used two separate combinations, i.e., 3.7-μm plus 1.6-μm channels and the 3.7-μm plus 2.1-μm channels, to retrieve two different DVPs. The final retrieved DVP was then the mean of the two. The bi-spectral retrieval approach can ease the

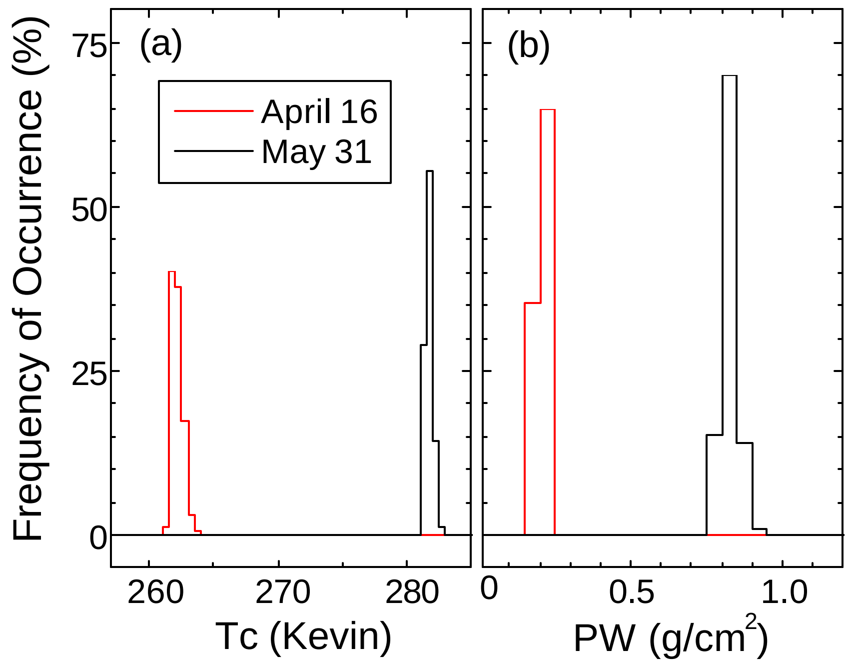

Figure 2. Frequency distributions of pixel-scale (a) T_c and (b) above-cloud PW obtained on April 16 and May 31, 2001, from a $(30\ km)^2$ area.

retrieval application as being more efficient than using all NIR channels simultaneously (cf., Chang and Li 2002), in regard to the generation of much less massive lookup tables from radiative transfer calculations. It significantly reduced the required computer executable memory size and computing time for the retrieval processes using MODIS data.

Note that the radiative transfer lookup tables were generated using an adding-doubling routine (Chang and Li 2002). The spectral reflectances and emissions were calculated using six values of above-cloud PW. Twelve T_g with a fixed lapse rate of $\Gamma = 6.5$ K/km were used for the atmospheric temperature profiles in the thermal radiation computations. The temperature for the tropopause was set to 216 K. Above the tropopause the U.S. standard atmospheric temperature profile was used. Other greenhouse gases were adopted from databases provided in the MODTRAN code. Molecular scattering was estimated based on the retrieved z_c. A Lambertian surface albedo of 0.2 was used for the three NIR channels and a value of 0.05 was used for the visible channel; this had little impact on the DVP retrievals for the thick stratus clouds considered here.

Figure 3 shows the three DVPs retrieved from the MODIS Level-1B 1-km data for the two stratus cloud cases studied here. Each sub-panel shows the retrieval means representing the three DVPs over a $(5\ km)^2$ area (black lines). The uncertainty of the mean is indicated by ± one standard deviation (although only showed for DVP2, they are similar in magnitude for the other two DVPs). Each group of four sub-panels represents a total area of $(10\ km)^2$ and sub-panel latitudes/longitudes from MODIS data are indicated. Generally speaking, the three MODIS-based DVP retrievals are similar in trend, with

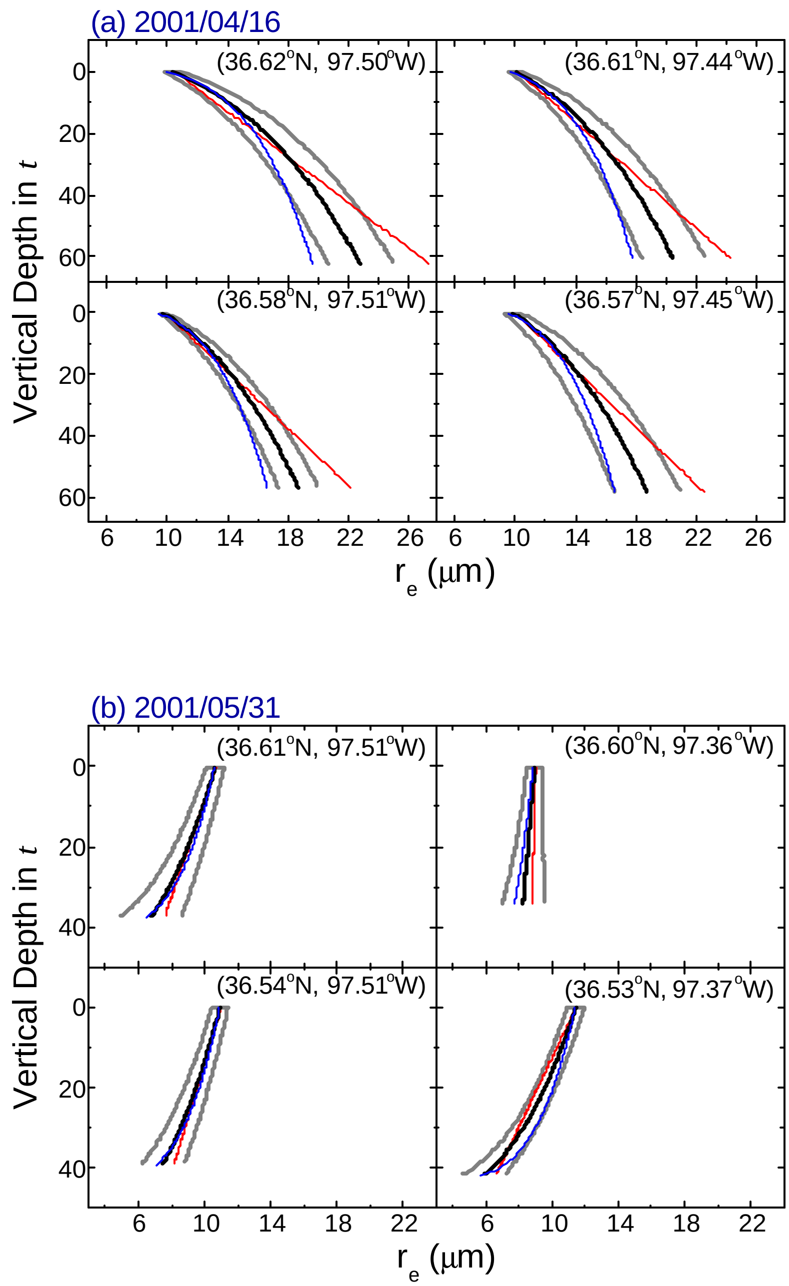

Figure 3. MODIS-retrieved DVPs using DVP1 (red), DVP2 (black), and DVP3 (blue) for (a) April 16 and (b) May 31, 2001. Each sub-panel showed retrievals obtained from a (5 km)^2 area, so a total area of (10 km)^2. Gray curves indicate the mean ± one standard deviation for the uncertainty of DVP2 retrieval. The uncertainty is similar in magnitude for DVP1 and DVP3 (not shown). Mean solar zenith, viewing zenith, and relative azimuth angles are (29.7°, 10.2°, 132°) for (a) and (24.4°, 53.2°, 155°) for (b).

increasing DER from cloud top to cloud bottom as shown in Figure 3a and decreasing DER from cloud top to cloud base as shown in Figure 3b. The difference in the vertical trend may help infer the development stage of a cloud, which can be potentially useful for studies concerning the aerosol indirect effects on clouds (Rosenfeld and Lensky 1998; Rosenfeld 2000). The three DVP retrievals are nearly the same in the upper portion of the profiles, but differences increase towards cloud bottom. This is understandable as the NIR channels are most sensitive to the cloud-top DER. Over all, their discrepancies are comparable to the local variability as indicated by ± one standard deviation (light-gray curves). The magnitudes of the standard deviations are similar for the three DVPs. These results are consistent with the uncertainty analysis presented in Chang and Li (2002).

Since the DVP2 falls in the middle of the three, it is recommended to use this profile if no other information indicates otherwise. Besides, the DER profile varying linearly with respect to height (DVP2) is observed most frequently from in-situ measurements (e.g., Miles et al. 2000). In the following section, some comparison on the retrieved DVP and liquid water path (LWP) with ground-based retrievals also focuses on this choice. Of course, if a cloud system is known to follow an adiabatic process, DVP3 shall be considered. Note that the retrievals shown in Figure 3 include only those pixels with a frequency distribution of τc between the 10th and 90th percentiles. Clockwise from the top left in each group of four sub-panels, the mean values of τ_c (standard deviation in parentheses) are 67.0 (10.4), 62.2 (9.8), 60.0 (9.7), 59.4 (4.6) for Figure 3a and 38.1 (2.2), 35.0 (3.4), 42.7 (4.4), 40.0 (3.6) for Figure 3b, which represent fairly uniform stratus cloud layers.

DER Vertical Profile versus LWP

LWP is calculated by integrating the LWC over a cloud column (i.e., LWP = $\int w(z')dz'$). Based on in-situ observations and modeling studies (e.g., Bower et al. 1994; Martin et al. 1994; Gultepe et al. 1996; Liu and Hallet 1997), relationship between LWC and droplet radius can be expressed as

$$w(z') = c_v\, r_v^3(z') = c_e\, r_e^3(z'), \tag{5}$$

where r_v is the volume mean radius of cloud droplets and c_v and c_e are taken to be constant by assuming a constant droplet number concentration with height (Chang and Li 2003).

The three analytic DVPs given in Equations 1 through 3 can also be rewritten in terms of z' (Platnick 2000) and given by

$$\text{DVP1:}\quad r_e(z') = [r_{e1}^{-1} + (r_{e2}^{-1} - r_{e1}^{-1})\, z']^{-1}, \tag{6}$$

$$\text{DVP2:}\quad r_e(z') = r_{e1} + (r_{e2} - r_{e1})\, z', \tag{7}$$

$$\text{DVP3:}\quad r_e(z') = [r_{e1}^3 + (r_{e2}^3 - r_{e1}^3)\, z']^{1/3}, \tag{8}$$

where $z' = (z - z_{top})/(z_{base} - z_{top})$ is the fractional height within cloud, r_{e1} represents r_e at $z' = 0$ for cloud top, and r_{e2} represents r_e at $z' = 1$ for cloud base. Assuming the extinction efficiency factor equals 2, the cloud optical depth at level z', $\tau(z')$, can be related to cloud LWC and DER by

$$t(z') \cong \frac{3}{2}\int_0^1 \frac{w(z')}{r_e(z')}dz' = \frac{3}{2}\int_0^1 c_e r_e^2(z')dz' \tag{9}$$

Thus, the value of c_e can be determined based on the retrievals of τ_c and DVP (viz. r_{e1} and r_{e2}). Note that conventional remote sensing applications commonly assume that r_e is independent of height; hence LWP was often approximated by

$$\mathrm{LWP} \approx 2/3\ \tau_c\ \overline{r_e}, \tag{10}$$

where $\overline{r_e}$ denotes the column mean DER. The resulting LWP is subject to a biased value pending on the DER profile. Note that in remote sensing applications, r_e often represents the shallow layer near the cloud top.

Figure 4 illustrates the MODIS-retrieved DVPs against the vertical depth in LWP by using DVP2 as shown in Figure 3 for the (10 km)^2 area. Because of variations in LWP from one pixel to another, the DVP retrievals were averaged in different ranges of LWP as shown in three separated sub-panels. Two ARM ground-based DVP retrievals are also plotted in the figure for comparisons, which were derived using two different ground-radar retrieval methods (Frisch et al. 1995; Dong and Mace 2003). Note that the two ground-retrievals show similar trend because both retrievals depend upon the radar reflectivity signals. The vertical depths are in column-integrated LWP from the cloud top ($z' = 0$) to different z-levels. It is seen that the MODIS-based and ground-based DVP retrievals are in good agreement with differences generally less than 2 μm, which is about the magnitude of the differences between the two radar retrievals. More importantly, the retrievals show similar trend of vertical variations. The retrieved mean LWPs were 604 g/m^2 (MODIS) and 535 g/m^2 (ground) for April 16 and 236 g/m^2 (MODIS) and 221 g/m^2 (ground) for May 31. In comparisons, the LWP values calculated using a constant r_e would be 420, 444, and 518 g/m^2 with respect to r_e = 10.3, 10.9, and 12.7 μm retrieved, respectively, from 3.7, 2.1, and 1.6-μm channels for April 16; and would be 275, 272, and 246 g/m^2 with respect to r_e = 10.7 (3.7-μm), 10.5 (2.1-μm), and 9.6 μm (1.6-μm) for May 31. Clearly, using a constant r_e tends to underestimate the LWP for an increasing DVP from cloud top to cloud base; and likewise, overestimate the LWP for a decreasing DVP. The over- or under-estimations are more severely with the more absorbing 3.7-μm channel.

Note that the focus of this paper is on modifications to a previously reported methodology and on demonstration of the performance of these modifications in retrieving the DVP. More comprehensive validation study is in progress, which will thoroughly evaluate the conditions that favor or disfavor the application of the method presented in this study and both its strengths and weaknesses (Chang et al. 2003).

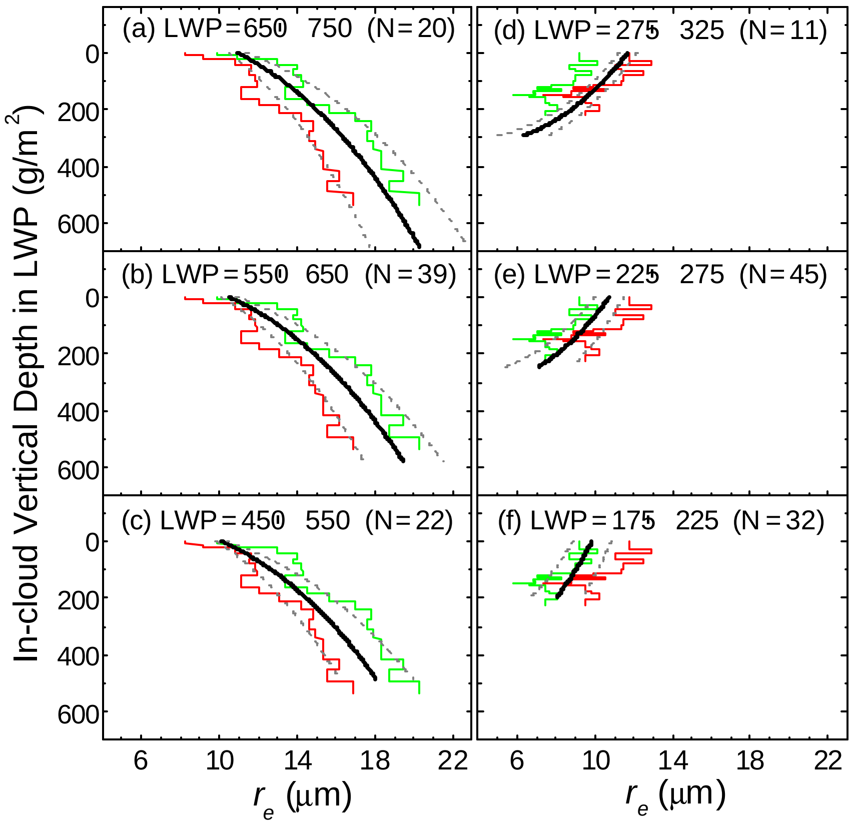

Figure 4. (a-c) Comparisons of MODIS-DVP2 (smooth curves) and ground (jagged) retrieved DVPs against the vertical depth in LWP (g/m^2) for April 4 and (d-f) May 31, 2001. Each sub-panel shows retrievals obtained from different range of LWP and N denotes the number of MODIS pixels sampled in the LWP range. MODIS retrievals are shown in mean (solid) ± one standard deviation (dashed) for the N pixels. Two ground retrievals were obtained with the Dong and Mace (solid) and Frisch et al. (dotted) schemes.

Concluding Remarks

Cloud DER is critically needed in climate studies. Information on the DER vertical structure is fundamental in understanding the interactions between clouds and aerosols and between clouds and the hydrology in the earth-atmosphere system. Conventional satellite remote sensing technique for retrieving the DER information has been limited to the retrieval of a vertically constant DER using a single NIR channel, which usually does not represent the whole cloud column. Here, we present a modified method to retrieve three types of DVP for boundary layer water clouds, assuming DVP being linear functions of in-cloud optical depth and height, as well a linear function of cloud water content with height. The three retrieval schemes were applied to the MODIS Level-1B 1-km radiance data. We also introduced a split window technique to better estimate precipitable water above a cloud.

As a preliminary assessment of the retrieval algorithm, DVPs, obtained from MODIS satellite-based and ARM ground-based measurements were compared at the SGP site in north central Oklahoma, with the latter serving as the "ground truth" on two days having uniform stratus clouds. The two sets of values are close in magnitude and the same in variation trend, attesting the soundness and robustness of the approach. It is also demonstrated that the enhanced DVP retrievals may provide more accurate estimates of LWP for boundary layer water clouds.

Acknowledgement

This research was supported by the U.S. Department of Energy Grant No. DE-FG02-01ER63166 under the Atmospheric Radiation Measurement Program.

Corresponding Author

Fu-Lung Chang, fchang@essic.umd.edu, (301) 405-5568

References

Bower, K. N., T. W. Choularton, J. Latham, J. Nelson, M. B. Baker, and J. Jensen, 1994: A parameterization of warm clouds for use in atmospheric general circulation models. *J. Atmos. Sci.*, **51**, 2722-2732.

Chang, F.-L., and Z. Li, 2003: Retrieving vertical profiles of water-cloud droplet effective radius: Algorithm modification and preliminary application. *J. Geophys. Res.*, submitted.

Chang, F.-L., and Z. Li, 2002: Estimating the vertical variation of cloud droplet effective radius using multispectral near-infrared satellite measurements. *J. Geophys. Res.*, **107**, AAC 7, 1-12

Chang, F.-L., Z. Li, and X. Dong, 2002: Validation of satellite-deduced vertical profile of cloud droplet effective radius using ground-based radar measurements. In *Proceedings of the Twelfth Atmospheric Radiation Measurement (ARM) Science Team Meeting*, ARM-CONF-2002. U.S. Department of Energy, Washington, D.C. Available URL:
http://www.arm.gov/docs/documents/technical/conf_0204/chang(1)-fl.pdf

Dong, X., T. P. Ackerman, and E. E. Clothiaux, 1998: Parameterizations of microphysical and shortwave radiative properties of boundary layer stratus from ground-based measurements. *J. Geophys. Res.*, **103**, 31,681–31,693.

Dong, X., and G. G. Mace, 2003: Profiles of low-level stratus cloud microphysics deduced from ground-based measurements. *J. Atmos. Oceanic Technol.*, **20**, 42-53.

Frisch, A., C. W. Fairall, and J. B. Snider, 1995: Measurement of stratus cloud and drizzle parameters in ASTEX with a K-band Doppler radar and a microwave radiometer. *J. Atmos. Sci.*, **52**, 2788–2799.

Gultepe, I., G. A. Isaac, W. R. Leaitch, and C. M. Banic, 1996: Parameterizations of marine stratus microphysics based on in situ observations: Implications for GCMs. *J. Climate*, **9**, 345-357.

Han, Q., W. B. Rossow, and A. A. Lacis, 1994: Near-global survey of effective droplet radii in liquid water clouds using ISCCP data. *J. Climate*, **7**, 465-497.

Hartmann, D. L., M. E. Ockert-Bell, and M. L. Michelsen, 1992: The effect of cloud type on the Earth's energy balance: Global Analysis. *J. Climate*, **5**, 1281-1304.

Kaufman, Y. J., and T. Nakajima, 1993: Effect of Amazon smoke on cloud microphysics and albedo–Analysis from satellite imagery. *J. Appl.Meteor.*, **32**, 729-744.

King, M. D., Y. J. Kaufman, W. P. Menzel, and D. Tanre, 1992: Remote sensing of cloud, aerosol, and water vapor properties from the moderate-resolution imaging spectrometer (MODIS). *IEEE Trans. Geosci. Remote Sens.*, **30**, 1-27.

King, M. D., W. P. Menzel, Y. J. Kaufman, D. Tanre, B. C. Gao, S. Platnick, S. A. Ackerman, L. A. Remer, R. Pincus, and P. A. Hubanks, 2003: Cloud and aerosol properties, precipitable water, and profiles of temperature and humidity from MODIS. *IEEE Trans. Geosci. Remote Sens*., in press.

Liu, Y., and J. Hallett, 1997: The "1/3" power-law between effective radius and liquid water content. *Quart. J. Roy. Meteor. Soc.*, **123**, 1789-1795.

Miles, N. L., J. Verlinde, and E. E. Clothiaux, 2000: Cloud droplet size distributions in low-level stratiform clouds, *J. Atmos. Sci.*, *57*, 295-311.

Nakajima, T. Y., and T. Nakajima, 1995: Wide-area determination of cloud microphysical properties from NOAA AVHRR measurements for FIRE and ASTEX regions. *J. Atmos. Sci.*, **52**, 4043-4059.

Platnick, S., and S. Twomey, 1994: Determining the susceptibility of cloud albedo to changes in droplet concentrations with the advanced very high resolution radiometer. *J. Appl. Meteorol*., **33**, 334-347.

Platnick, S., 2000: Vertical photon transport in cloud remote sensing problems. *J. Geophys. Res.*, **105**, 22,919-22,935.

Stephens, G. L., 1999: Radiative effects of clouds and water vapor, in *Global Energy and Water Cycle*, K. A. Browning and R. J. Gurney, Eds., pp. 71-90, Cambridge Univ. Press, New York.